ISSN 0208-7774 TRIBOLOGIA 4/2023 p. 43–51
DOI: 10.5604/01.3001.0054.3942

Piotr OSADA[*], Marcin KOT[**], Sławomir ZIMOWSKI[***], Grzegorz WIĄZANIA[****], Jürgen LACKNER[*****]

ADAPTIVE DLC COATINGS WITH DIFFERENT MoS_2 CONTENT

POWŁOKI ADAPTACYJNE DLC O RÓŻNEJ ZAWARTOŚCI MoS_2

Key words: anti-wear self-lubricating chameleon coatings, tribotest, friction, high temperature.

Abstract: DLC coatings are widely used in engineering as they are resistant to abrasive wear. However, they exhibit an increased coefficient of friction at temperatures of around 300°C. Soft MoS_2 coatings are known to maintain a low coefficient of friction at temperatures up to about 350°C, but suffer from relatively high abrasive wear. Publications from the last decade report a synergistic improvement in the tribological performance of a coating consisting of both these materials. The aim of this study was to investigate the wear resistance of coatings composed of different a-C and MoS_2 contents applied by magnetron sputtering on steel. The results obtained in tribological tests conducted using the ball-and-disk method showed at least 20% better adhesion to the substrate of the two-component nanocomposite coating and its increased wear resistance from 15% to as much as 700%, compared to single-component coatings in tests conducted at 20°C and 250°C. The tests showed no deterioration of the two-component coating's coefficient value compared to DLC.

Słowa kluczowe: przeciwzużyciowe kameleonowe powłoki samosmarujące, tribotest, tarcie, wysoka temperatura.

Streszczenie: Powłoki DLC znajdują szerokie zastosowanie w technice, ponieważ są odporne na zużycie ścierne. Jednak wykazują podwyższony współczynnik tarcia w temperaturach rzędu 300°C. Miękkie powłoki MoS_2 są znane z utrzymywania niskiego współczynnika tarcia w temperaturach do około 350°C, jednak ulegają relatywnie dużemu zużyciu ściernemu. Publikacje z ostatniej dekady podają synergiczne polepszenie parametrów tribologicznych powłoki składającej się z obu tych materiałów. Celem pracy było badanie odporności na zużycie powłok złożonych z różnej zawartości a-C i MoS_2 nanoszonych techniką rozpylania magnetronowego na stali. Wyniki uzyskane w testach tribologicznych prowadzonych metodą kula–tarcza wykazały co najmniej 20% lepszą przyczepność do podłoża dwuskładnikowej powłoki nanokompozytowej oraz jej zwiększoną trwałość na zużycie ścierne od 15% do nawet 700%, porównując z jednoskładnikowymi warstwami w badaniach prowadzonych w temperaturze 20°C i 250°C. Badania nie wykazały pogorszenia wartości współczynnika powłoki dwuskładnikowej w porównaniu do DLC.

INTRODUCTION

Coatings applied to various substrates have long been widely used as one of the forms of creating surface properties. Depending on the expectations placed on the components, different coatings and different application methods are used. They can have different functions: coloring, corrosion protection, surface texture modification; electrical:

[*] ORCID: 0000-0002-9176-983X. AGH University of Science and Technology, Faculty of Mechanical Engineering and Robotics, Al. Mickiewicza 30 Ave., 30-059 Krakow, Poland, e-mail: kotmarc@agh.edu.pl.
[**] ORCID: 0000-0002-3017-9481. AGH University of Science and Technology, Faculty of Mechanical Engineering and Robotics, Al. Mickiewicza 30 Ave., 30-059 Krakow, Poland, e-mail: kotmarc@agh.edu.pl.
[***] ORCID: 0000-0002-7348-8751. AGH University of Science and Technology, Faculty of Mechanical Engineering and Robotics, Al. Mickiewicza 30 Ave., 30-059 Krakow, Poland, e-mail: kotmarc@agh.edu.pl.
[****] ORCID: 0000-0001-9247-0015. AGH University of Science and Technology, Faculty of Mechanical Engineering and Robotics, Al. Mickiewicza 30 Ave., 30-059 Krakow, Poland, e-mail: kotmarc@agh.edu.pl.
[*****] ORCID: 0000-0003-3931-232X. Joanneum Research Forschungsgesellschaft GmbH., Institute for Sensors, Photonics and Manufacturing Technologies, Leobner Straße 94, A-8712 Niklasdorf, Austria.

conductivity of electrical charge; and inertness to react with other chemicals. Some of the important surface characteristics are mechanical properties, as well as tribological properties such as coefficient of friction or resistance to abrasive wear.

Among the large group of anti-wear coatings, DLC (*Diamond-Like Carbon*) coatings are of interest. In electronics, the use of DLC coatings on HDD platters has helped to increase their resistance to scratching by the read/write head and to corrosion. For this reason, the durability of the platter-head pair has increased 50–200 times **[L. 1].** Further enhancements in thin DLC coatings have reduced the distance between the platter and the head, allowing for the denser distribution of the magnetic domains that store information **[L. 2]**.

Obtaining adequate abrasion resistance and coefficient of friction at a certain required level can be difficult under changing environmental conditions, such as varying temperatures. One group of coatings that can meet these requirements are adaptive coatings, otherwise known as chameleon coatings. Such coatings can be obtained by combining materials with significantly different properties, each of which individually exhibiting only certain tribological characteristics desirable under extreme operating conditions. Key features of frictional cooperation are the coefficient of friction (CoF) and the wear index (W_V). Examples of machine parts operating under the types of conditions where adaptive coatings could be applied are shaft journals in internal combustion engines **[L. 3]**, combustion chamber valves **[L. 4]**, and piston rings **[L. 5]**, etc.

DLC carbon coatings have been successfully applied to such components to date. They make it possible to reduce the coefficient of friction by 11% and increase the friction node's resistance to seizure in internal combustion engine shaft journals **[L. 3]**. In addition to strictly mechanical properties, modifying the surface of engine components with DLC coatings can affect the combustion process. Thus, the power characteristics of the engine and the composition of the emitted exhaust gas are altered. The coating of combustion chamber valves contributes to a 3–7% reduction in fuel consumption and a 20–35% reduction in harmful emissions **[L. 4]**. Meanwhile, a cylinder face coating has enabled a 2.5% reduction in specific fuel consumption **[L. 6]**. The use of multilayer coatings with a top layer made of DLC on ceramic cutting inserts, with the top layer made of DLC, makes it possible to increase the durability of such inserts by up to 60–80% **[L. 7, 8]**.

They are also used in bioengineering due to, among other things, to their low thrombogenicity. For this reason, the DLC surface prevents the formation of blood clots. On the other hand, the biocompatibility of this surface promotes the growth of cells of organisms, such as endothelium in arteries and veins. This property allows the DLC surface to grow over tissue. As a result, diamond-like coatings are widely used as covering materials for endoprostheses **[L. 9–12]**. DLC coatings also make it possible to increase the hardness of surgical instrument blades **[L. 13]**.

DLC exhibits mechanical properties between *graphite* and *diamond*, which highly depend on the ratio of plane bonds sp^2 and tetragonal bonds sp^3 between carbon atoms **[L. 14]**. The sp^2 bonds are weaker than sp^3 ones. The sp^2 hybridization creates carbon in a graphitic structure, while the sp^3 bonds are responsible for the properties of diamond resulting in high hardness. On the other hand, the graphitic structure provides a hexagonal structure, so that slippage between crystal planes becomes possible **[L. 14]**. This slip mechanism is used in solid lubricants. The proportions between bond types significantly affect the characteristics of DLC (hardness, Young's modulus E, coefficient of friction CoF, wear index W_v). DLC coatings with an appropriate bonding ratio are characterized by high hardness, high abrasion wear resistance, low coefficient of friction, and they are optically transparent **[L. 15]**. Regarding temperature, DLC with low content of sp^3 bindings (circa 10%) can be degraded by the impact of temperature as low as 200°C **[L. 16]**.

One combination of materials with promising results in frictional cooperation over a wide temperature range (from room temperature to 250°C) that can be used as an alternative to DLC coatings for the components in the examples cited earlier are chameleon coatings, composed of DLC in the form of amorphous carbon (a-C) in combination with molybdenum disulfide (MoS_2).

The MoS_2 material is successfully used in practice for piston ring coatings. Deposition on piston rings with molybdenum disulfide makes it possible to reduce the frictional force of the piston against the cylinder by 40% compared to chromium-plated tribological coatings **[L. 17]**.

Wear tests of the MoS_2 coating performed in a temperature range from 20°C to 120°C showed

a decrease in wear with increasing temperature **[L. 18]**. This is the opposite trend to DLC coatings, where an increase in wear with growing temperature is observed due to graphitization (change in bond type) **[L. 19]**. For the described coatings made of MoS_2 and a-C, a decrease in friction coefficient with increasing temperature was observed **[L. 18]**, **[L. 19]**.

In view of the great potential for the application of a-C/MoS_2 chameleon coatings to machine components operating in a wide temperature range and the lack of knowledge regarding their properties in frictional cooperation, the determination of the basic tribological characteristics of this type of coating was undertaken. Therefore, in this study, the values of wear index and coefficient of friction were determined for a-C coatings with different proportions of MoS_2 and compared to single MoS_2 and a-C coatings during dry friction at temperatures of 23°C and 250°C.

The suitability of coatings for use in machine friction nodes operating at elevated temperatures is determined by mechanical and chemical properties. The mechanical properties, wear resistance and coefficient of friction are the most important. These quantities can be determined by standardized tribological tests **[L. 20]**. The damage mechanisms of the coatings, primarily related to adhesion to the substrate, are also very important. These can be investigated using the scratch test. It allows the determination of load values at which cohesive cracks (within the coating material), adhesion cracks (detachment of coating fragments from the substrate) and delamination (complete detachment of the coating from the substrate) appears **[L. 20]**, **[L. 21]**. Another quantity characterizing the coating-substrate system is the hardness determined in the indentation test and, with a suitable model, the indentation modulus of elasticity can also be determined in this test **[L. 20–23].**

The results of the described tests provide a basis for inferring the suitability of a given coating for use in a specific friction node. In particular, these parameters are used to estimate features important from the operational point of view, such as durability, resistance to motion, resistance to cracking and delamination of coatings and the related unfavorable appearance of wear products in the friction zone, as well as the load-bearing capacity of the coating-substrate system in concentrated contact.

The aim of this work is to analyze mechanical and tribological properties of a-C/MoS_2 nanocomposite coatings at ambient and 250ºC temperatures. The performance of these coatings was compared with a-C and MoS_2 monolithic coatings. As none of these single coatings has both low coefficient of friction and wear index at two above-mentioned temperatures, we proposed composites of both materials.

RESEARCH MATERIALS AND METHODS

The subjects of the study were composite coatings composed of amorphous carbon a-C and molybdenum disulfide MoS_2. Groups of materials with the following substance ratios of the individual compounds were tested:

- 100% a-C,
- 90% a-C + 10% MoS_2,
- 50% a-C + 50% MoS_2,
- 100% MoS_2.

Coatings were deposited by magnetron sputtering in an industrial chamber (Leybold, Cologne, Germany) with 4 rectangular magnetrons with a size of 3 "x17" and a maximum power of 3kW. The substrates were X5CrNi18-10 austenitic stainless-steel plates with a thickness of 1.5 mm and dimensions of 20×20 mm. The substrates were polished to a mirror shine and ultrasonically washed in acetone and ethanol before deposition of the coatings. The carbon a-C and molybdenum disulfide MoS_2 coatings were deposited in an argon atmosphere by spraying a disc of graphite and sintered MoS_2 powder, respectively. For the deposition of a-C/MoS_2 composite coatings, four discs (two each of carbon and MoS_2) were deposited simultaneously.

Abrasion resistance was determined after tribological tests in a sliding ball-disk contact geometry (**Fig. Fig. 2**). A T-21 tribotester produced by the Łukasiewicz Research Network – Institute for Sustainable Technologies in Radom was used for the tests, with a temperature chamber enabling tribological tests to be conducted at temperatures up to 750°C **[L. 24, 25]**. The value used to evaluate the wear resistance of the tested samples was the volumetric wear index, calculated according to equation (1) **[L. 26]**:

$$W_V = \frac{V}{F_N \cdot s}\left[\frac{mm^3}{N \cdot m}\right] \quad (1)$$

where: V – volume of the material removed from the surface in the friction process, FN – force of

the counterexample on the surface, and s – friction path. The volume of the material removed was determined from the three-dimensional profile (**Fig. 1**). Parameters used during the tribological tests were sa follows: countersample – a sphere made of alumina (Al_2O_3) with a diameter of 6 mm; normal load of 1 N; chamber temperature RT (room temperature 23±2°C) and 250°C stabilized within ±2°C according to the standard **[L. 27]**; disc speed 120 rpm; number of cycles: 20,000 (revolutions); and number of experimental repetitions: 3. For each material and temperature conditions, tests were carried out on separate samples at different radii: 4, 5, 6 mm (all of the three wear tracks on the same specimen).

Scratch tests were performed using an Anton Paar MCT micro-combi tester[3] (**Fig. 4(a)**) employing a Rockwell diamond indenter with a spherical tip with a radius of 200 µm. The critical load Lc3 was adopted for the comparative evaluation of the coating's adhesion to the substrate. This is the load at which the coating completely detaches from the substrate. The tests were performed in a linearly increasing normal force from 0 N to a maximum force of 30 N, with the indenter moving across the surface at 5 mm/min speed within a 5 mm length (**Fig. 3**).

Nanohardness was determined using an instrumental method on an Anton Paar NHT nanoindenter[3]. The test involved pressing an indenter with Berkovich geometry, and the Oliver-Pharr method was used to analyze the measurement data **[L. 22, 28–31].** Measurements were carried out with the following parameters: maximum force F_{max} = 2 mN, loading and unloading speed 4 mN/s, maximum load holding time 5 s.

These settings were selected to ensure penetration depths are between 5% and 10% of the coating thickness. Since penetration depths are less than 10% of the coating thickness, it can be assumed that the substrate material has no influence on the measured hardness **[L. 22, 29]**. The hardness value was calculated using the equation (2) **[L. 29]**:

$$H = \frac{F_{max}}{A_p(h_c)}\left[MPa\right] \tag{2}$$

Where: H_{IT} – indentation hardness; F_{max} [N] – maximum force loading the indenter; A_p (h_c) [mm^2] – surface drop of the indentation made by the indenter at depth h_c (cross-section of the indenter in the plane perpendicular to the direction of force application); h_c [mm] – depth of contact of the indenter with the specimen at force F_{max}.

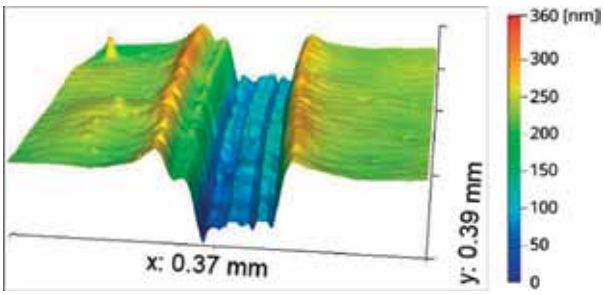

Fig. 1. Three-dimensional model of a furrow used to determine the volume of the removed material and the average profile of wear tracks

Rys. 1. Przykładowy model trójwymiarowy bruzdy służący do wyznaczenia objętości zużytego materiału i średniego profilu wytarcia

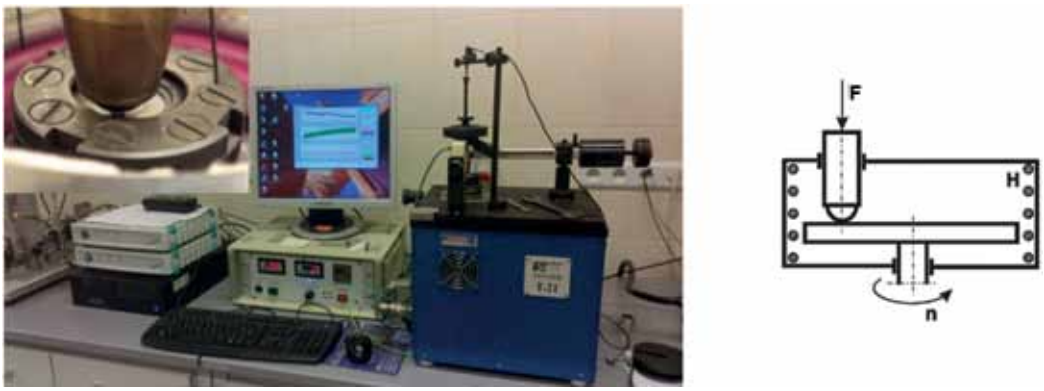

Fig. 2. Friction wear test bench and schematic of a ball-disc test system with a temperature-controlled heating chamber [L. 24]. F – contact force, H – heat source, n – rotational speed

Rys. 2. Stanowisko do testów zużycia ciernego i schemat układu badawczego typu kula-tarcza z komorą grzewczą o regulowanej temperaturze **[L. 24]**. F – siła nacisku, H – źródło ciepła, n – prędkość obrotowa

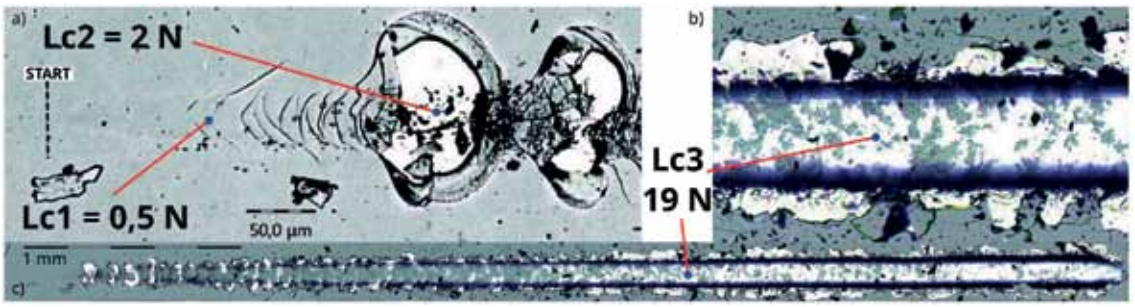

Fig. 3. Example of specimen scratching with a maximum force of 30 N over a length of 5 mm (steel substrate)
Rys. 3. Przykładowe zarysowanie próbki z siłą maksymalną 30 N na długości 5 mm (podłoże stalowe)

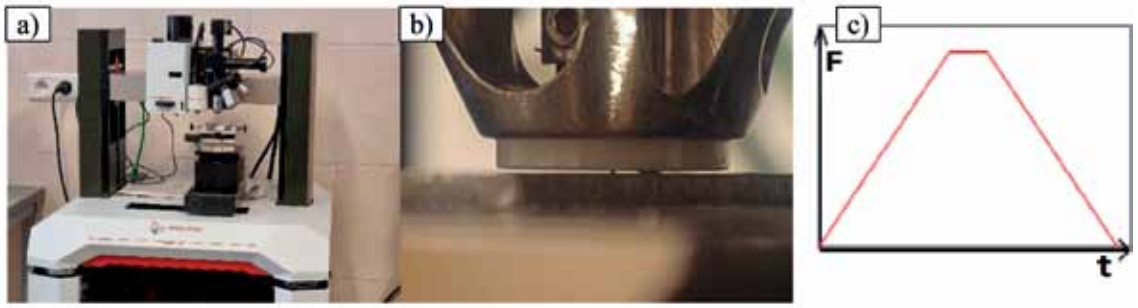

Fig. 4. Anton Paar Step 500 platform with NHT³ attachment for nanoindentation and MCT³ attachment for nano-scale scratch and indentation test: a) NHT head³ approaching the surface, b) Schematic of the indenter load time course c) [L. 32]
Rys. 4. Platforma Anton Paar Step 500 z przystawką NHT3 do nanoindentacji i MCT3 do testu zarysowania i indentacji w skali nano: a) głowica NHT3 zbliżająca się do powierzchni, b) schemat przebiegu obciążenia wgłębnika w czasie c) **[L. 32]**

RESULTS

After scratch testing, the results showed that for coatings made of pure a-C and pure MoS_2, the critical load causing the coating to completely detach from the substrate Lc3 was at the same level of 24–25 N. The nanocomposite with 50% MoS_2 showed adhesion lower by 25%. In contrast, the a-C + 10% MoS_2 coating did not detach when the maximum load available on the measuring device (30 N) was applied. For the other coatings, the load at which detachment from the substrate occured (Lc3) was about 25% lower (**Tab. 1**). The wear index values obtained from the tribological tests at RT and 250°C and the nanohardness of the tested coatings, measured for a force of 2 mN are presented in **Table 1**.

Table 1. Mechanical and tribological test results: nanohardness, scratch resistance (Lc3) and mean volumetric wear index with standard deviation (SD)
Tabela 1. Wyniki testów mechanicznych i tribologicznych: nanotwardość, odporność na zarysowanie (Lc3) i średni objętościowy wskaźnik zużycia z odchyleniem standardowym (SD)

Coating material	Coating thickness [µm]	H_{IT} (2 mN) [GPa]	Lc3 [N] *1	$W_V \left[10^{-6} \cdot \frac{mm^3}{N \cdot m}\right]$		CoF [-] *2	
				Temp. RT	250°C	RT	250°C
a-C	3.45	**10.5** (SD:2.8)	24	**0.68** (SD:0.17)	**1.36** (SD:0.34)	**0.077** (SD:0.028)	**0.053** (SD:0.019)
a-C + 10% MoS_2	4.10	**12.2** (SD:2.2)	>30 *3	**0.31** (SD:0.02)	**1.15** (SD:0.45)	**0.079** (SD:0.024)	**0.032** (SD:0.011)
a-C + 50% MoS_2	2.65	**6.4** (SD:0.43)	19	**0.98** (SD:0.20)	**1.82** (SD:0.50)	**0.145** (SD:0.027)	**0.018** (SD:0.006)
MoS_2	3.40	**3.7** (SD:1.1)	25	**2.10** (SD:0.63)	**5.21** (SD:1.00)	**0.213** (SD:0.042)	**0.018** (SD:0.009)

[1] Failure modes specific to Lc1 and Lc2 critical loads are not present in every coating.
[2] The value of the coefficient of friction is the average value from the period in which the coatings were not removed.
[3] For the maximum force achievable on the Anton Paar MST³, which is 30 N, no mechanism of separation of the coating from the substrate (delamination) was observed.

Wear test results show that in all tests carried out at room temperature RT=23°C, the molybdenum disulfide coatings maintain continuity for up to about 14,000 cycles. For 16,000–17,000 cycles, the coating is abraded and further friction of the Al_2O_3 ball is observed in cooperation with the austenitic substrate X5CrNi18-10. The other coatings maintain stable friction conditions throughout the test (20,000 cycles). At elevated temperatures, the pure a-C coating is abraded during the initial period of cooperation (**Fig. Fig. 6**). With the exception of the 100% a-C coating, the friction process, in contact with the alumina ball, at 250°C occurs with less resistance than at room temperature (**Fig. 5** and **6**).

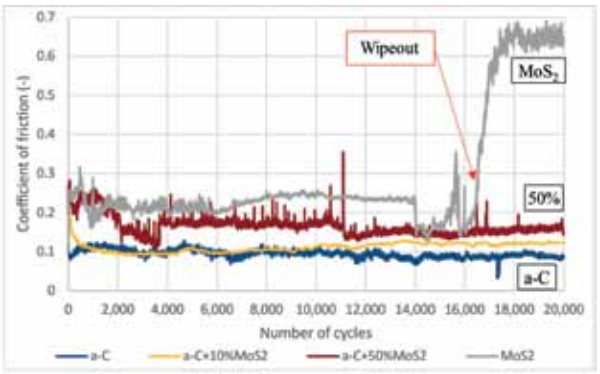

Fig. 5. Selected coefficient of friction characteristics at room temperature

Rys. 5. Wybrane przebiegi współczynnika tarcia w temp. pokojowej

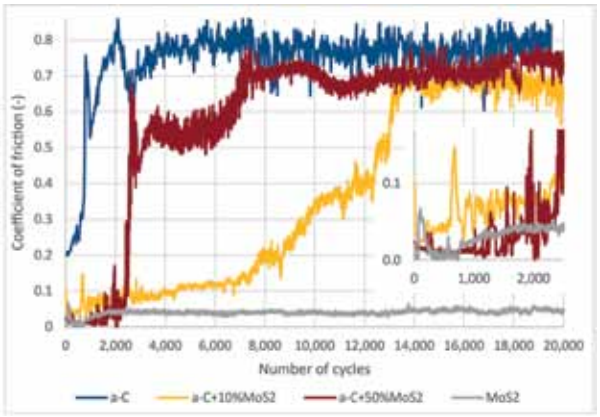

Fig. 6. Coefficient of friction at 250°C

Rys. 6. Współczynnik tarcia w temp. 250°C

At low temperature, a strong correlation can be observed between an increase in the proportion of MoS_2 in the coating and the average value of the coefficient of friction (CoF = 0.08 for 100% a-C and CoF = 0.20 for 100% MoS_2). However, at 250°C each coating shows a lower coefficient of friction than at RT (0.05). The frictional force is lower the higher the proportion of molybdenum disulfide in the coating. In contact with a 100% MoS_2 coating, CoF = 0.05 at a steady state (**Fig. 6**).

Higher temperatures accelerate the frictional wear process of a-C/MoS_2 coatings. Every coating tested shows a higher wear rate at 250°C than at 23°C. Wear intensity at elevated temperatures increases in the range of 80% to 270% for individual coatings (**Tab. Tab. 1**). A graph of the wear cross-section is shown in **Fig. Fig. 7**. Coatings of the a-C/MoS_2 type show small fluctuations in friction force values during normal operation. **Fig. Fig. 5** shows that, in the case of the MoS_2 coating, the rubbing stage of the coating is associated with a significant reduction in the frictional force. Complete rubbing occurred when the coefficient of friction stabilized at around 0.7, which is a characteristic value for a steel-ceramic alumina pair in non-lubricated sliding contact.

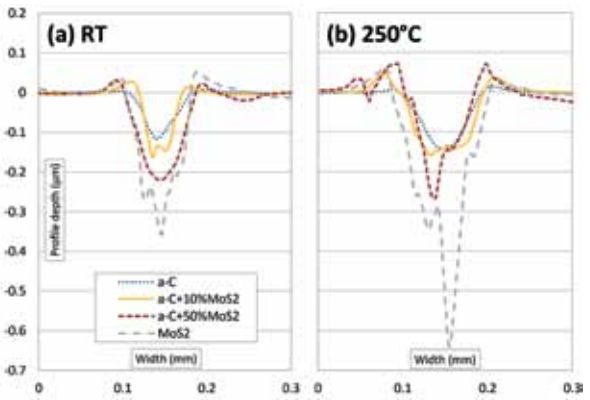

Fig. 7. Wear track profiles of the tested coatings at room temperature and 250°C

Rys. 7. Profile wytarcia badanych powłok w temperaturze pokojowej i 250°C

The results show that there is a relationship between the wear resistance of the coatings and their hardness. The hardest coating (a-C + 10% MoS_2) showed the highest wear resistance. And the least hard coating (MoS_2) showed the lowest wear resistance (cf. **Tab. 1**).

The tests carried out in contact with the alumina ball showed, that at room temperature all coatings, except 100% MoS_2 were not abraded after 20,000 friction cycles. However, at elevated temperature, only the 100% MoS_2 coatings did not rub off after this number of cycles. Closer to this result in terms of durability is the number of friction cycles of an alumina countersample in contact with the a-C + 10% MoS_2 coating. The period of stable operation in this case was approximately 7,000 cycles.

The 100% a-C coating, despite its relatively high hardness, was abraded very early at 250°C. Its hardness of 10.4 GPa and high peel resistance (Lc3 = 24 N, Rockwell 200 μm) are not matched by high abrasion resistance. In contrast, at room temperature, the coating did not abrade in any of the 20,000 friction cycles tested. The 100% a-C coating was not abraded at 23°C and showed low abrasive wear intensity W_V of 0.68 (RT) and 1.36 (250°C) [10^{-6} $mm^3N^{-1}m^{-1}$]. The tribological characteristics of the coating in question show that, at 250°C, the 100% a-C coating was abraded after several hundred to several thousand friction cycles in the three tests carried out.

The distinguishing feature of the 100% MoS_2 coating is the low coefficient of friction at 250°C of 0.03. This material showed the lowest stable CoF value of all the coatings tested. Such low values occur at elevated temperatures. At room temperature, the frictional resistance of the MoS_2 coating in contact with the Al_2O_3 ball remained at the highest level throughout the experiment (CoF = 0.2). Similar results were also obtained in the work by A. Jiang et al. **[L. 33]**. The 100% MoS_2 coating shows good adhesion - it detaches at a force of 25 N. For this coating, the hardness is the lowest (H_{IT} = 3.8 GPa) and the wear intensity was found to be the highest among the materials tested at both RT and 250°C. At both temperatures, the W_V value was at least twice as high as for the other coatings. Despite the highest wear rate value, the 100% MoS_2 coating was the only one that did not rub off at 250°C after 20,000 friction cycles. Instead, the MoS_2 coating did not maintain its continuity in the friction process at room temperature for the planned number of cycles. It was rubbed off after approximately 14,000 cycles.

The a-C + 50% MoS_2 coating showed the lowest coefficient of friction at 250°C of the order of 0.01, but only in the initial phase of the test (2,000 cycles). After further friction cycles, it quickly rubbed off. The coating has rather low adhesion to the substrate at Lc3 = 19 N. For this reason, a-C + 50% MoS_2 is the least suitable for use in systems where high coating cohesion is required.

Of the coatings tested, a-C + 10% MoS_2 showed the highest scratch resistance (Lc3 exceeds the measurement range of the apparatus used - 30 N). Its hardness is 16% higher than that of a-C alone, and wear rates are at the lowest level at both temperatures used. The coating shows most of the parameters determining durability and slip resistance with Al_2O_3 at the best level for use as an anti-wear coating. This results in low friction resistance. Despite the observed abrasion of a-C + 10% MoS_2 coatings in the range of approximately 7,000 to 18,000 cycles, this coating composition appears to be optimal for use as a sliding coating.

SUMMARY

The measurement methods used made it possible to determine the frictional cooperation capabilities of a-C/MoS_2 nanocomposite coatings under constant room temperature and 250°C conditions. The results of the conducted tests indicate that the coating with a-C + 10% MoS_2 has the most favorable arrangement of tribological parameters in terms of low coefficient of friction (CoF) and low abrasive wear (W_V), combined with high coating adhesion to steel and low susceptibility to fracture. The a-C + 10% MoS_2 coating wears at more than twice the rate of 100% MoS_2 at RT. In contrast, at 250°C the coating with 10% MoS_2 is 15% less abrasive than 100% a-C and almost five times less than 100% MoS_2. The coefficient of friction of Al_2O_3–a-C + 10% MoS_2 tribopair is 0.10–0.12 at room temperature and 0.05–0.10 at 250°C. The resistance in the scratch test exceeds Lc3 = 30 N compared to 24, 19 and 25 N for 100% a-C, a-C + 50% MoS_2 and 100% MoS_2, respectively.

ACKNOWLEDGMENT

This work was supported by the Polish Ministry of Education and Science under the subvention fund of the Department of Machine Design and Exploitation of AGH-UST (AGH grant number 16.16.130.942).

REFERENCES

1. Bogy D.B., Yun X., Knapp B.J.: Enhancement of head-disk interface durability by use of diamond-like carbon overcoats on the slider's rails, IEEE Trans. Magn., vol. 30, no. 2, pp. 369–374, Mar. 1994, doi: 10.1109/20.312289.

2. Puttichaem C., Souza G.P., Ruthe K.C., Chainok K.: Characterization of Ultra-Thin Diamond-Like Carbon Films by SEM/EDX, Coatings, vol. 11, no. 6, Art. no. 6, Jun. 2021, doi: 10.3390/coatings11060729.
3. Ogihara H., Iwata T., Mihara Y., and Kano M.: The effects of DLC-coated journal on improving seizure limit and reducing friction under engine oil lubrication, Int. J. Engine Res., p. 14680874211012934, Apr. 2021, doi: 10.1177/14680874211012934.
4. Sivakumar E.R., Senthilkumar P., Sreenivasan M., and Krishna R.: Experimental investigation of H-DLC coated exhaust valve characteristics of a diesel engine, Mater. Today Proc., vol. 33, pp. 675–681, Jan. 2020, doi: 10.1016/j.matpr.2020.05.776.
5. Vinoth I.S., Detwal S., Umasankar V., and Sarma A.: Tribological studies of automotive piston ring by diamond-like carbon coating, Tribol. - Mater. Surf. Interfaces, vol. 13, no. 1, pp. 31–38, Jan. 2019, doi: 10.1080/17515831.2019.1569852.
6. Rejowski E.D., Mordente P. Sr, Pillis F.M., Casserly T.: Application of DLC Coating in Cylinder Liners for Friction Reduction, presented at the SAE 2012 World Congress & Exhibition, Apr. 2012, pp. 2012–01–1329. doi: 10.4271/2012-01-1329.
7. Grigoriev S., Volosova M., Fyodorov S., Lyakhovetskiy M., and Seleznev A.: DLC-coating Application to Improve the Durability of Ceramic Tools, J. Mater. Eng. Perform., vol. 28, no. 7, pp. 4415–4426, Jul. 2019, doi: 10.1007/s11665-019-04149-1.
8. Grigoriev S. et al.: Nanostructured Multilayer Composite Coatings for Cutting Tools, in Advanced Ceramic Materials, Mhadhbi M., Ed., IntechOpen, 2020, p. 22. doi: 10.5772/intechopen.94363.
9. Bociaga D. et al.: Surface Characteristics and Biological Evaluation of Si-DLC Coatings Fabricated Using Magnetron Sputtering Method on Ti6Al7Nb Substrate, Nanomaterials, vol. 9, no. 6, Art. no. 6, Jun. 2019, doi: 10.3390/nano9060812.
10. Dearnaley G. and J.H. Arps: Biomedical applications of diamond-like carbon (DLC) coatings: A review, Surf. Coat. Technol., vol. 200, no. 7, pp. 2518–2524, Dec. 2005, doi: 10.1016/j.surfcoat.2005.07.077.
11. Rajak D.K., Kumar A., Behera A., and Menezes P.L.: Diamond-Like Carbon (DLC) Coatings: Classification, Properties, and Applications, Appl. Sci., vol. 11, no. 10, Art. no. 10, Jan. 2021, doi: 10.3390/app11104445.
12. Jastrzębski K., Jastrzębska A., and Bociąga A.: A review of mechanical properties of diamond-like carbon coatings with various dopants as candidates for biomedical applications, Acta Innov., vol. 22, pp. 40–57, 2017.
13. Kadlec J., Joska Z., and Kadlec J.: Study of Biocompatible ZrN and ZrN/DLC Coating Deposited on Medical Tools, ECS Trans., vol. 48, no. 1, p. 315, Jan. 2014, doi: 10.1149/04801.0315ecst.
14. Robertson J.: Diamond-Like Carbon Films, Properties and Applications, in Comprehensive Hard Materials, Elsevier, 2014, pp. 101–139. doi: 10.1016/B978-0-08-096527-7.00043-X.
15. Khan K.A. and Khan M.I.: Enhancement the graphitic nature of DLC by Au doping and incorporation of 300 keV Ni2+ ions in DLC thin films, Mater. Res. Express, vol. 6, no. 6, p. 066413, Mar. 2019, doi: 10.1088/2053-1591/ab0e49.
16. Braak R. et al.: Accelerated thermal degradation of DLC-coatings via growth defects, Surf. Coat. Technol., vol. 349, pp. 272–278, Sep. 2018, doi: 10.1016/j.surfcoat.2018.05.063.
17. Di Y., Cai Z., and Zhang P.: The Tribological Performance of CrMoN/MoS2 Solid Lubrication Coating on a Piston Ring, Lubricants, vol. 5, no. 2, Art. no. 2, Jun. 2017, doi: 10.3390/lubricants5020013.
18. Serles P., Gaber K., Pajovic S., Colas G., and Filleter T.: High Temperature Microtribological Studies of MoS2 Lubrication for Low Earth Orbit, Lubricants, vol. 8, no. 4, Art. no. 4, Apr. 2020, doi: 10.3390/lubricants8040049.
19. Kot M. et al.: Adaptive coatings a-C/MoS2, Tribologia, vol. 278, no. 2, pp. 51–56, May 2018, doi: 10.5604/01.3001.0012.6975.
20. Menezes P. L., Ingole S.P., Nosonovsky M., Kailas S.V. , and Lovell M.R., (Eds.): Tribology for scientists and engineers: from basics to advanced concepts. New York: Springer, 2013.
21. Kutilek P. and Miksovsky J.: The procedure of evaluating the practical adhesion strength of new biocompatible nano- and micro-thin films in accordance with international standards, Acta Bioeng. Biomech., vol. 13, no. 3, pp. 87–94, 2011.

22. Fischer-Cripps A.C.: Nanoindentation, 3rd ed. in Mechanical Engineering Series. New York, NY: Springer New York, 2011. doi: 10.1007/978-1-4419-9872-9.
23. Fischer-Cripps A.C.: The IBIS handbook of nanoindentation, 1st ed. Forestville, NSW: Fischer-Cripps Laboratories Pty Ltd., 2013. Accessed: Jan. 19, 2021. [Online]. Available: http://www.fclabs.com.au/index_htm_files/IBIS_HandbookOfNanoindentationBook.pdf.
24. ITE Radom: Urządzenie T-21 typu kula-tarcza. Do tribologicznych badań materiałów konstrukcyjnych w wysokiej temperaturze. ITE Radom. Accessed: Jul. 06, 2022. [Online]. Available: https://www.tribologia.org/ptt-old/inst/rad/T-21.pdf
25. Michalak M., Michalczewski R., and Wulczyński J.: Modyfikacja tribologicznego urządzenia badawczego T-21 przeznaczonego do badania materiałów w wysokiej temperaturze, Tribologia, no. 6, pp. 79–95, 2014.
26. ISO 20808:2004 Fine ceramics (advanced ceramics, advanced technical ceramics) – Determination of friction and wear characteristics of monolithic ceramics by ball-on-disc method, International Organization for Standardization, Standard, Feb. 2004. Accessed: Apr. 08, 2022. [Online]. Available: https://www.iso.org/standard/65415.html.
27. ISO 18535:2016, Mar. 2016. Accessed: Jul. 25, 2022. [Online]. Available: https://cdn.standards.iteh.ai/samples/62820/4f883ab72002481e887d5126291f4d21/ISO-18535-2016.pdf.
28. Bhushan B. and Palacio M.L.B.: Nanoindentation, in Encyclopedia of Nanotechnology, B. Bhushan, Ed., Dordrecht: Springer Netherlands, 2016, pp. 2423–2444. doi: 10.1007/978-94-017-9780-1_41.
29. ISO 14577-1:2015 Metallic materials – Instrumented indentation test for hardness and materials parameters – Part 1: Test method, International Organization for Standardization, Standard, Jul. 2015. Accessed: Apr. 08, 2022. [Online]. Available: https://www.iso.org/standard/56626.html.
30. Lucca D.A., Herrmann K. and Klopfstein M.J.: Nanoindentation: Measuring methods and applications, CIRP Ann., vol. 59, no. 2, pp. 803–819, Jan. 2010, doi: 10.1016/j.cirp.2010.05.009.
31. Oliver W.C. and. Pharr G.M: An improved technique for determining hardness and elastic modulus using load and displacement sensing indentation experiments, J. Mater. Res., vol. 7, no. 6, pp. 1564––1583, Jun. 1992, doi: 10.1557/JMR.1992.1564.
32. Reference Guide. Step X00 - NHT3. Nanoindentation Tester. Anton Paar TriTec SA, Jan. 2020.
33. Jiang A., Cao X., Wang Z., Ma J., Xiao J., and Ma S.: Friction performance and corrosion resistance of MoS2/DLC composite films deposited by magnetron sputtering, Results Phys., vol. 25, p. 104278, Jun. 2021, doi: 10.1016/j.rinp.2021.104278.